

Functional and Structural Roles of the Highly Conserved Trp120 Loop Region of Glucoamylase from *Aspergillus awamori*

Sateesh Natarajan and Michael R. Sierks*

Department of Chemical and Biochemical Engineering, University of Maryland Baltimore County, Baltimore, Maryland 21228

Received October 17, 1995; Revised Manuscript Received December 13, 1995[®]

ABSTRACT: The functional role of a loop region, highly conserved among glucoamylase and other starch hydrolases which also includes the essential Trp120 of *Aspergillus awamori*, is investigated. Residues 121–125 of *A. awamori* glucoamylase were singly substituted, and their individual effects on catalytic activity and thermal stability were determined. The Arg122→Tyr mutation displayed opposing effects for shorter and longer maltooligosaccharide substrates, K_m decreasing for shorter substrates but increasing for longer substrates. The Pro123→Gly mutation decreases the thermal stability of glucoamylase by 19 °C with little effect on activity. The Gln124→His substitution decreases k_{cat} for all substrates 10–15-fold. Gly121→Thr and Arg125→Lys had only minor effects on glucoamylase activity. While Arg122→Tyr, Gln124→His, and the previously constructed Trp120→Phe [Sierks, M. R., Svensson, B., Ford, C., & Reilly, P. J. (1989) *Protein Eng.* 2, 621–625] glucoamylases have significantly reduced activity toward maltose hydrolysis, all mutations in the Trp120 loop region retain wild-type level activity toward α -D-glucosyl fluoride hydrolysis. The Trp120 loop region therefore plays a major role in directing conformational changes controlling the postulated rate-limiting product release step, even though only Trp120 is indicated to interact with acarbose in the crystal structure [Aleshin, A. E., Firsov, L. M., & Honzatko, R. B. (1994) *J. Biol. Chem.* 269, 15631–15639]. Side chains of residues 116, 120, 122, and 124 oriented in one direction play crucial roles in the enzyme mechanism, while side chains of residues 119, 121, 123, and 125, oriented in the opposite direction, play only minor roles.

Glucoamylase (GA)¹ (1,4- α -D-glucan glucohydrolase, EC 3.2.1.3) is an exohydrolase which cleaves D-glucose from the nonreducing ends of starch and related oligo- and polysaccharides (Hiromi et al., 1983). GA hydrolyzes both α -1,4- and α -1,6-glucosidic linkages at a single active site (Hiromi et al., 1966a), although the α -1,4 linkages are cleaved much more readily than the α -1,6 linkages.

Two carboxyl groups have been implicated in the GA catalytic mechanism (Hiromi et al., 1966b; Savel'ev & Firsov, 1982). Hydrolysis is postulated to proceed by a general acid catalyst donating a hydrogen to the oxygen of the scissile glycosidic bond and a catalytic base promoting the nucleophilic attack of a water molecule on the C-1 carbon of the aglycon moiety. Glu179 of *Aspergillus awamori* GA has been identified as the general acid catalyst and Glu400 as the catalytic base group based on mutagenesis and crystallographic studies (Sierks et al., 1990; Harris et al., 1993; Aleshin et al., 1994a,b; Frandsen et al., 1994).

The crystal structure of GA from *A. awamori* GA, Var X-100 shows a catalytic domain consisting of 13 α -helices, 12 of which are arranged in a polypeptide fold dubbed as an α/α barrel (Aleshin et al., 1994a). The active site is located in the packing void of the α/α barrel, as evident from the crystal structures of GA complexed with inhibitors 1-deoxynojirimycin and acarbose (Harris et al., 1993; Aleshin et al., 1994b). Comparison of primary sequences from 15 yeast and fungal GA sequences indicate five highly conserved regions (Itoh et al., 1987; Coutinho & Reilly, 1994; Henrissat et al., 1994). Each of these conserved regions

occurs as a loop element connecting the structural α -helices and form much of the active site pocket (Harris et al., 1993).

One of these regions which includes the Trp120 residue of *A. awamori* GA also shares substantial similarity with other enzymes active on glucosidic linkages (Svensson, 1988; Sierks et al., 1992). In GA, residues 115–125 form a nonstructural loop located primarily on the surface and bordering one side of the active site as seen from the crystal structures (Harris et al., 1993; Aleshin et al., 1994b). The three-dimensional crystal structure of two of the related enzymes, a cyclodextrin glucanotransferase (CGTase) (Klein & Schulz, 1991) and Taka-amylase (Matsuura et al., 1984), indicate that the homologous regions in these enzymes are also part of a long nonstructural loop adjacent to the active site similar to the structure and location of the GA Trp120 loop. A third related enzyme, glucose oxidase (Hecht et al., 1993), also contains a structurally similar loop in the active site. Glucose oxidase, which oxidizes glucose to glucono- δ -lactone, is more distantly related than the other enzymes since it does not act on oligosaccharides. The GA catalytic mechanism, however, is considered to involve a glucono- δ -lactone type intermediate (László et al., 1978), so the sequence similarity between GA and Glucose oxidase may be associated with stabilization of intermediates resembling glucono- δ -lactone.

The Trp120 of *A. awamori* GA plays a critical role in GA activity. Chemical modification studies suggested Trp120 is situated near subsite 4 (Clarke & Svensson, 1984b). Site-directed mutagenesis and subsequent kinetic analysis indicated that Trp120 is involved in transition-state stabilization (Sierks et al., 1989) and interacts with the active site (Sierks

* Address correspondence to this author.

[®] Abstract published in *Advance ACS Abstracts*, February 15, 1996.

¹ Abbreviations: GA, glucoamylase; GF, α -D-glucosyl fluoride.

et al., 1990). Steady-state fluorescence perturbation studies indicated that Trp120 undergoes substantial conformational change upon substrate binding (Svensson & Sierks, 1992), and stopped-flow fluorescence spectroscopic experiments with Trp120→Phe GA suggest that Trp120 also plays a significant part in directing necessary conformational changes in the enzyme upon initial substrate recognition (Olsen et al., 1993). The GA crystal structure shows a hydrogen bond between NE1 of Trp120 and OE2 of Glu179, the general acid catalyst (Aleshin et al., 1994a). Kinetic analyses using α -D-glucopyranosyl fluoride as a substrate with various GA mutants suggest Trp120 plays a key role in the product release mechanism (Sierks & Svensson, 1996).

Even though the catalytic domains of GA and the related carbohydrases have different super secondary structures, the similar local folding patterns in the Trp120 region may indicate similar functional roles. Trp84 of *Saccharomycopsis fibuligera* α -amylase, the residue equivalent to Trp120 of *Aspergillus niger* GA, has been located at subsite 3 of the enzyme and plays a role in liberating the product from the binding pocket (Matsui et al., 1991). The Trp120 loop is therefore not only critical in the GA catalytic mechanism but also plays important roles in other carbohydrases. To further probe the role of this critical Trp120 region in the GA catalytic mechanism, site-directed mutations were constructed at residues 121–125 of *A. awamori* GA, and the effects of the mutations on enzyme activity and stability were determined. A variety of substrates were used including two disaccharide substrates, maltose (α -1,4 linkage) and isomaltose (α -1,6 linkage), a series of α -1,4-linked linear malto-oligosaccharides from maltotriose to maltoheptaose, and α -D-glucosyl fluoride. The disaccharides are used to detect changes in linkage specificity and the maltooligosaccharides for changes in any of the seven subsites of GA. With oligosaccharide substrates, the reducing end sugar residues can remain unproductively bound to the active site after hydrolysis reducing the enzyme turnover rate. α -D-Glucosyl fluoride has no such residue and was used as a substrate to probe whether release of the reducing end product limits the overall reaction rate for natural substrates.

MATERIALS AND METHODS

Rationale for Design of GA Mutants. The mutations at residues 121–125 of *A. awamori* GA were based on sequence comparison of 15 GA sequences and sequences of related α -amylases, CGTase, and glucose oxidase (Figure 1). The residues at positions 121–124 are strictly conserved in the fungal glucoamylases while the residue at position 125 is Arg or Asn. Substitutions at Gly121, Arg122, Gln124, and Arg125 were based on the occurrence of a different residue in one or more of the other related enzymes. Therefore Gly121→Thr was designed to make GA resemble glucose oxidase and maltogenic α -amylase. The Arg122→Tyr mutation was designed to probe the role of this residue in substrate linkage specificity since GAs, maltogenic α -amylase, CGTase, and glucose oxidase all have an Arg at position 122, while the α -1,6-hydrolyzing enzymes have a Tyr. A variety of side chains are present at position 124 in the related enzymes, so Gln124→His was constructed based on the glucose oxidase sequence. Arg125→Lys was constructed since CGTase, maltogenic α -amylase, and glucose oxidase have a Lys at position 125 while the GAs have a similar but longer Arg or Asn side chain. At position 123, proline is

Glucoamylase	112	-	D	E	T	A	Y	T	G	S	W	G	R	P	Q	R	D ^a
CGT-ase	93	-	T	N	T	A	Y	H	G	Y	W	A	R	D	F	K	K ^b
Maltogenic α -amylase	85	-	D	N	T	G	Y	H	G	Y	W	T	R	D	F	K	Q ^c
Fungal α -amylase	75	-	Y	F	D	A	Y	T	G	Y	W	Q	T	D	I	Y	S ^a
Yeast α -amylase	100	-	T	A	Y	G	Y	H	G	Y	W	M	K	N	I	Y	K
Isoamylase	246	-	N	S	D	A	N	Q	N	Y	W	G	Y	M	T	E	N ^c
Pullulanase	547	-	V	A	Q	T	D	S	Y	N	W	G	Y	D	P	F	H ^c
Glucose Oxidase	103	-	S	T	L	V	N	G	G	T	W	T	R	P	H	K	A ^d

FIGURE 1: Amino acid sequence similarities between enzymes active on glucose or chains of α -linked glucosyl residues. The aligned sequences are identified by a number representing the location of the first residue appearing in the sequence counting from the amino terminus of the mature protein. The highlighted residue characters represent alignments where at least six of the eight sequences have similar residues. Glucoamylase residues 121–125, shown as boxed, are residues studied in this work. Glucoamylase, *Aspergillus niger* (Svensson et al., 1983); fungal α -amylase, *Aspergillus niger* (Matsuura et al., 1984); yeast α -amylase, *Saccharomycopsis fibuligera* (Itoh et al., 1987); maltogenic α -amylase, *Bacillus stearothermophilus* (Diderichsen & Christiansen, 1988); cyclodextrin glucanotransferase (CGTase), *Bacillus circulans* (Klein & Schulz, 1991); isoamylase, *Pseudomonas amyloclavata* (Ame-mura et al., 1988); pullulanase, *Klebsiella aerogenes* (Katsuragi et al., 1987); glucose oxidase, *Aspergillus niger* (Fredrick et al., 1990). Alignments are taken from ^a(Svensson, 1988), ^b(McGregor & Svensson, 1989), ^c(Jespersen et al., 1993), and ^d(Sierks et al., 1992).

conserved in all the GAs and in glucose oxidase. Since proline has the least conformational freedom, the Pro123→Gly mutation was designed to study the effects of a more flexible residue at this position. The mutations were based on sequence comparison since the X-ray crystallographic structure of GA was not available at the time.

Production and Purification Of Mutant Enzymes. A *Xho*I–*Sal*I–*Pst*I fragment of the GA gene, containing the coding region for residues 121–125 of *A. awamori* GA, was subcloned into the pBluescript KSII+ vector to facilitate genetic manipulations (Sierks et al., 1989; Cole et al., 1988). Mutations were introduced into the *Sal*I–*Pst*I fragment using polymerase chain reaction with specifically designed oligonucleotide primers and the T7 universal primer. The oligoprimers were designed to contain the mutated codon and also to introduce new silent restriction sites for mutations of residues 121–124 and delete an already existing *Ava*II site for residue 125. The following oligonucleotide primers were used (mutations are denoted by boldface type and the new silent restriction sites are underlined):

Gly121→Thr 5'-TTCAATGTCGAGAGACTGCCTAC-
ACTGGATCCTGGACACGGCCGCAGCG-3'

Arg122→Tyr 5'-CTACACTGATCCTGGGGGTACCC-
GCAGCGAGA-3'

Pro123→Gly 5'-CTACACTGGATCCTGGGGGACG-
TGGCCAGCGAGAG-3'

Gln124→His 5'-TACACTGGATCCTGGGGGCGGCC
GCATCGAGATGG-3'

Arg125→Lys 5'-hTCCTGGGGGCGGCCGCAGAAAGG-
ATGGCCCG-3'

The *Sal*I–*Pst*I fragments containing the desired mutations were verified by DNA sequencing (Sanger et al., 1977). The *Xho*I–*Sal*I–*Pst*I mutant fragments were then subcloned into the GA gene in the shuttle vector YEpm18 replacing the wild-type fragment.

Table 1: Kinetic Parameters for Wild-Type and Mutant Glucoamylases at 45 °C, pH 4.5

substrate	wild type		Gly121→Tyr		Arg122→Tyr	
	k_{cat} (s ⁻¹)	K_m (mM)	k_{cat} (s ⁻¹)	K_m (mM)	k_{cat} (s ⁻¹)	K_m (mM)
isomaltose	0.34 ± 0.01	30.3 ± 1.2	0.34 ± 0.01	21.6 ± 2.1	0.025 ± 0.000	13.2 ± 0.6
maltose	9.2 ± 0.4	1.4 ± 0.20	4.0 ± 0.08	1.62 ± 0.12	0.275 ± 0.002	0.77 ± 0.03
maltotriose	38.7 ± 1.5	0.52 ± 0.06	22.6 ± 0.3	0.30 ± 0.04	0.98 ± 0.03	0.25 ± 0.03
maltotetraose	49.1 ± 2.2	0.31 ± 0.04	45.6 ± 2.5	0.17 ± 0.02	2.97 ± 0.10	0.48 ± 0.06
maltopentaose	49.2 ± 2.5	0.22 ± 0.03	48.8 ± 2.5	0.13 ± 0.02	5.70 ± 0.29	0.61 ± 0.10
maltohexaose	46.2 ± 1.7	0.16 ± 0.02	50.7 ± 2.2	0.13 ± 0.02	5.05 ± 0.21	0.55 ± 0.07
maltoheptaose	54.1 ± 1.6	0.13 ± 0.01	53.2 ± 2.5	0.12 ± 0.02	5.71 ± 0.10	0.83 ± 0.06

substrate	Gln124→His		Arg125→Lys		Tyr116→Ala ^a	
	k_{cat} (s ⁻¹)	K_m (mM)	k_{cat} (s ⁻¹)	K_m (mM)	k_{cat} (s ⁻¹)	K_m (mM)
isomaltose	0.033 ± 0.001	14.5 ± 1.7	0.61 ± 0.02	17.8 ± 1.6	0.111 ± 0.005	23.2 ± 3.0
maltose	0.63 ± 0.03	0.737 ± 0.062	6.69 ± 0.10	0.61 ± 0.05	0.62 ± 0.02	0.57 ± 0.05
maltotriose	2.32 ± 0.02	0.224 ± 0.016	13.3 ± 0.62	0.23 ± 0.03	0.53 ± 0.02	0.028 ± 0.004
maltotetraose	4.24 ± 0.09	0.119 ± 0.009	26.8 ± 1.44	0.19 ± 0.03	16.6 ± 1.1	0.51 ± 0.09
maltopentaose	4.29 ± 0.16	0.099 ± 0.014	20.9 ± 0.80	0.12 ± 0.01	19.1 ± 0.5	0.24 ± 0.02
maltohexaose	4.65 ± 0.19	0.126 ± 0.019	18.3 ± 0.66	0.11 ± 0.01	22.2 ± 0.7	0.26 ± 0.03
maltoheptaose	4.55 ± 0.09	0.091 ± 0.005	21.0 ± 0.8	0.13 ± 0.01	23.6 ± 1.2	0.29 ± 0.02

^a From Sierks and Svensson (1996).

Competent cells of *Saccharomyces cerevisiae* C468 strain were prepared for transformation using lithium acetate (Ito et al., 1983). Transformed cells were grown in a 20 L New Brunswick Scientific Bioflo IV fermenter with 15 L working volume at 30 °C and pH 4.5 for 72 h in selective medium containing 6.7 g/L of Difco Bacto yeast nitrogen base without amino acids, 2% glucose, 5 g/L ammonium sulfate, and 100 mg/L histidine (Cole et al., 1988). Glucose was replenished after 48 h of fermentation (Chen et al., 1994). Cells were removed by centrifugation and the supernatant concentrated to 2 L using a Millipore Pellicon system and further concentrated 40-fold using a Millipore Minitan system (10 000 molecular weight cutoff filters). GA was purified using a Sepharose-Acarbose affinity column and eluted as described previously (Clarke & Svensson, 1984b). Eluted enzyme was dialyzed against water and lyophilized. All purification steps were performed at 4 °C.

Glucoamylase Kinetic Assays. Protein concentrations were determined using OD 280nm with extinction coefficients of $\epsilon_m = 1.37 \times 10^5 \text{ M}^{-1} \text{ cm}^{-1}$ and $\epsilon_m = 1.30 \times 10^5 \text{ M}^{-1} \text{ cm}^{-1}$ for wild type and Trp120→Phe GA, respectively (Clarke & Svensson, 1984a). All kinetic assays were performed at 45 °C in 0.05 M sodium acetate buffer, pH 4.5, except for analyses of Pro123→Gly GA which were performed at 25 °C due to the decreased thermal stability of this enzyme. The series of linear α -1,4-linked D-glucosyl oligosaccharide substrates from maltose to maltoheptaose and the α -1,6-linked disaccharide, isomaltose, were purchased from Sigma (St. Louis, MO). Kinetic data were obtained as described using at least seven substrate concentrations ranging from 8 times above to 8 times below K_m (Frandsen et al., 1994). Enzyme concentrations in the reaction mixtures ranged from 0.003 to 0.77 μM for wild-type GA, 0.003 to 1.0 μM for Gly121→Thr GA, 0.03 to 1.75 μM for Arg122→Tyr GA, 0.008 to 1.8 μM for Pro123→Gly GA, 0.01 to 0.39 μM for Gln124→His GA, and 0.003 to 0.50 μM for Arg125→Lys GA. The rates were determined by removing aliquots and measuring the concentrations of the released glucose by the glucose oxidase method as modified for microtiter plate assays (Fox & Robyt, 1991; Palcic et al., 1993). Kinetic parameters, k_{cat} and K_m , of the Michaelis–Menten equation were obtained by nonlinear regression of initial rates vs

substrate concentration using Grafit (Leatherbarrow, 1992).

Crystalline α -D-glucosyl fluoride (GF) was a generous gift from Professor Inge Lundt (Danish Technical Institute, Lyngby, Denmark). GF substrates were prepared in 0.05 M sodium acetate buffer, pH 4.5, stored at 4 °C, and used within 12 h. The GF samples were found to contain about 5% glucose just prior to the assay. GF hydrolysis at pH 4.5 was followed using four concentrations (0.5, 1, 1.5, and 2 mM) of GF sufficiently low to ensure that the rate (v) was proportional to k_{cat}/K_m . Enzyme concentrations, chosen to ensure the total glucose concentration did not exceed 10% of initial GF concentration during the course of the assay, were as described above. An enzyme concentration of 0.013 μM was used for Trp120→Phe GA. Reaction rates were measured by monitoring the concentrations of the released glucose as described above. The nonenzymic hydrolysis of GF to glucose was determined to be negligible during the time course of the assay. Limited substrate availability did not permit calculation of the individual k_{cat} and K_m values.

Thermal Stability Studies. Irreversible thermal inactivation of Pro123→Gly GA was determined by incubating the enzyme in 0.05 M sodium acetate buffer, pH 4.5, at incremental temperatures between 25 and 75 °C for different time periods ranging from 0 to 60 min and assaying for residual activity using 20 mM maltose as substrate at 25 °C. The first-order rate coefficients of thermal inactivation, k_d , were calculated at each temperature by linear regression of a plot of \ln (residual activity) vs incubation time (Chen et al., 1994). Residual activity of Pro123→Gly and wild-type GAs after 10 min of incubation at various temperatures were used to calculate the denaturation temperature, T_m , of the enzymes.

RESULTS AND DISCUSSION

The kinetic parameters, k_{cat} and K_m , obtained for Gly121→Thr, Arg122→Tyr, Gln124→His, Arg125→Lys, and wild-type GAs at 45 °C are listed in Table 1 and for Pro123→Gly and wild type GAs at 25 °C are listed in Table 2. The free energy of formation of a transition-state complex for an enzyme-catalyzed reaction is reflected in its (k_{cat}/K_m) value (Fersht, 1985). The difference in the binding energy

Table 2: Kinetic Parameters for Wild-Type and Pro123→Gly Glucoamylases at 25 °C, pH 4.5

substrate	wild type ^a		Pro123→Gly	
	k_{cat} (s ⁻¹)	K_m (mM)	k_{cat} (s ⁻¹)	K_m (mM)
isomaltose	0.06	25.0	0.038 ± 0.002	29.33 ± 3.23
maltose	2.20	0.56	1.41 ± 0.02	0.52 ± 0.03
maltotriose	8.90	0.19	5.80 ± 0.28	0.24 ± 0.04
maltotetraose			7.62 ± 0.30	0.11 ± 0.01
maltopentaose			9.22 ± 0.40	0.10 ± 0.01
maltohexaose			9.89 ± 0.37	0.07 ± 0.01
maltoheptaose			7.95 ± 0.49	0.06 ± 0.01

^a Values read from a graph (Meagher et al., 1989a) with an estimated error of 10% or less.

between the transition-state complex stabilized by wild type and a mutated enzyme can be calculated using the equation (Wilkinson et al., 1983)

$$\Delta(\Delta G) = -RT \ln[(k_{\text{cat}}/K_m)_{\text{mutant}}/(k_{\text{cat}}/K_m)_{\text{wt}}]$$

where $\Delta(\Delta G)$ measures the change in free energy of the transition state complex for the rate-determining step. The $\Delta(\Delta G)$ values calculated for each mutant enzyme for hydrolysis of each of the maltooligosaccharides and isomaltose are listed in Table 3. The effect of each of these mutations on the GA mechanism will be discussed individually.

Gly121→Thr. Despite being strictly conserved in the 15 different GA sequences, the presence of Gly at position 121 is not crucial for GA activity. There was little change in the k_{cat} values obtained with the various substrates as compared to wild-type GA, except for a 2-fold decrease seen for maltose and maltotriose hydrolysis. The K_m values decrease slightly for all substrates except maltose which has a value similar to wild type. The similar kinetic parameters and small $\Delta(\Delta G)$ values obtained for isomaltose hydrolysis indicate that the mutation does not affect activity toward the α -1,6 linkage. The specificity for maltose (G2) over isomaltose (iG2) hydrolysis as indicated by the ratio $[k_{\text{cat}}/K_m]_{\text{G2}}/[k_{\text{cat}}/K_m]_{\text{iG2}}$ is 4-fold lower for the mutant than for wild type due to a decrease in maltose specificity. The small increase in free energy for maltose hydrolysis resulting from the mutation (2.6 kJ/mol) without a change in K_m suggests that Gly121 plays a minor role in transition-state stabilization but not in enzyme complex formation. Substitution of Gly with Thr may hinder the flexibility of the protein backbone in this region and decrease the ability of the mutant enzyme to stabilize the transition state as suggested by the crystal structure of GA-acarbose complex (Aleshin et al., 1994b) which locates Gly121 near the second subsite.

Arg122→Tyr. The Arg122→Tyr substitution has very substantial effects on the GA catalytic parameters and shows specific differences in activity toward shorter and longer maltooligosaccharides. The k_{cat} values obtained for maltose and maltotriose hydrolysis decrease 33- and 39-fold, respectively, compared to wild type, while the values for longer substrates are just 16–9-fold lower. The ratio of maltose (G2) to maltoheptaose (G7) turnover rates, as reflected in $[(k_{\text{cat}})_{\text{G2}}/(k_{\text{cat}})_{\text{G7}}]$, for the mutant is 21 compared to 6 for wild type. The large decrease in k_{cat} for short substrates is linkage specific as k_{cat} for isomaltose hydrolysis decreases only 14-fold compared to wild type, similar to the longer substrates. The difference in activity between shorter and longer

substrates caused by this mutation is even more pronounced in the K_m values. For wild-type GA, K_m for maltooligosaccharide hydrolysis decreases consistently from 1.4 to 0.13 mM as the substrate chain length increases from two to seven. The K_m values obtained with Arg122→Tyr GA decrease from maltose to maltotriose but then increase for the longer substrates. Compared to wild type, the K_m values obtained with maltose and maltotriose for the mutant enzyme decrease 2-fold, while those for maltotetraose, maltopentaose, maltohexaose, and maltoheptaose hydrolysis increase 2-, 3-, 4-, and 6-fold, respectively. The decrease in K_m value with short substrates is not linkage specific in this case as the value for isomaltose hydrolysis also decreases 2-fold compared to wild type.

This distinction between short and long substrates has only been observed in one other GA mutation to date, Tyr116→Ala GA (Sierks and Svensson, 1996). The kinetic parameters for Tyr116→Ala GA are qualitatively similar to Arg122→Tyr GA and are listed in Table 1 for comparison. The increases in K_m values for the longer substrates with both mutant enzymes are accompanied by substantial increases in k_{cat} . Comparing maltotetraose to maltotriose hydrolysis, a 2-fold increase in K_m accompanies a 3-fold increase in k_{cat} for Arg122→Tyr GA, and an 18-fold increase in K_m accompanies a 31-fold increase in k_{cat} for Tyr116→Ala GA. The 1.5-fold larger increase in k_{cat} over K_m indicates that both these mutant enzymes increase their turnover rates by destabilizing ground state complexes. The destabilization of the bound complexes for both the Arg122→Tyr and Tyr116→Ala GAs beginning with maltotetraose and longer substrates suggest that GA residues 116 and 122 are both situated around or influence subsite 4 although neither of these two residues are in the immediate vicinity of the inhibitor residues in the GA-acarbose crystal structure (Aleshin et al., 1994b). This apparent conflict between the results of kinetic studies in solution and the crystal structures is discussed later. The NH₂ atom of Arg122 is, however, hydrogen-bonded to carbonyl oxygen of Tyr116 in the crystal structure indicating these residues may be functionally linked.

The Arg122→Tyr mutation destabilizes the transition state by 8–11 kJ/mol for hydrolysis of the α -1,4-linked substrates and 5 kJ/mol for isomaltose hydrolysis as reflected in the $\Delta(\Delta G)$ values. Tyr116→Ala GA has a much smaller effect on the transition state, increasing $\Delta(\Delta G)$ values from 3 to 5 kJ/mol for the α -1,4-linked substrates and about 2 kJ/mol for isomaltose. Since the $\Delta(\Delta G)$ values obtained for all the α -1,4-linked substrates are similar, the transition-state complexes for all the maltooligosaccharide substrates for both these enzymes are not differentially affected. The increase in turnover rates with increasing substrate lengths, therefore, is primarily due to a decrease in stabilization of the ground-state complexes for the longer substrates or to an increase in ground-state stabilization with the short substrates as illustrated by the strong binding between maltotriose and Tyr116→Ala GA.

Gln124→His. This mutation also significantly affects the catalytic parameters. The k_{cat} values obtained with Gln124→His for hydrolysis of all the substrates decrease between 10- and 15-fold compared to wild-type GA, while the corresponding K_m values decrease 1.5–2.0-fold resulting in $\Delta(\Delta G)$ values for all the substrates of around 5 kJ/mol. The decrease in K_m reflects increased formation of bound enzyme complexes, while the decrease in k_{cat} reflects a slower

Table 3: Changes in the Binding Energy of the Transition State Complexes [$\Delta(\Delta G)$ kJ/mol] between Wild-Type and Mutant Glucoamylases

substrate	Gly121→Thr	Arg122→Tyr	Gln124→His	Arg125→Lys	Tyr116→Ala ^a
isomaltose	0.8	4.7	4.2	-3.0	+2.1
maltose	2.6	7.8	5.4	-1.3	+4.7
maltotriose	0.0	7.8	5.2	0.7	+3.6
maltoetraose	1.2	8.6	4.0	0.3	+4.2
maltopentaose	1.3	8.4	4.3	0.7	+2.9
maltohexaose	0.7	9.1	5.4	1.4	+3.3
maltoheptaose	0.2	10.9	5.6	2.3	+4.3

^a From Sierks and Svensson (1996).

turnover, the combination indicating the mutation stabilizes one or more ground-state enzyme complexes which subsequently increases the magnitude of the activation energy barrier.

The crystal structure of GA-acarbose complex shows NE2 of Gln124 hydrogen bonded to OE2 of Glu179, the catalytic acid residue (Aleshin et al., 1994b). In addition, the OE1 of Gln124 also shares a bidentate hydrogen bond with NH1 of Arg54. This is part of a complex hydrogen-bonding network surrounding the first and second subsites of the enzyme. The δ and ϵ nitrogen, of the imidazole ring of His124, if properly positioned, could still conceivably retain hydrogen bonding to Arg54 and Glu179 as seen with wild-type GA. The bulky histidine ring, however, could disrupt the hydrogen-bonding network and result in destabilization of the transition-state complex. The similar $\Delta(\Delta G)$ values of about 5 kJ/mol observed for all the substrates could be due to perturbation of the very specific hydrogen-bonding network or to some displacement of Glu179.

Arg125→Lys. The conservative substitution of Lys for Arg did not have very large effects on the catalytic parameters. The k_{cat} value for maltose hydrolysis decreases approximately 25% relative to wild type, while the k_{cat} values for the longer α -1,4-linked substrates decrease from 2.5- to 3.0-fold. The K_m values obtained for all the α -1,4-linked substrates are about half of the corresponding values for wild type, again indicating increased formation of bound enzyme complexes. The k_{cat} value for isomaltose hydrolysis increases about 2-fold compared to wild type, in contrast to the decreased activity toward the α -1,4 linkages, while K_m decreases about 2-fold. The 4-fold increase in isomaltose specificity decreases the selectivity for maltose over isomaltose hydrolysis from nearly 600 for wild-type GA to 320.

The $\Delta(\Delta G)$ values for the Arg125→Lys GA indicate that a lysine at position 125 causes some favorable interactions specifically for disaccharides stabilizing the isomaltose and maltose transition state by nearly 3 and 1.3 kJ/mol, respectively. The transition-state energies for hydrolysis of the substrates maltotriose to maltoheptaose in contrast show smaller increases. Maltose and isomaltose have very different ground-state and transition-state structures in GA (Olsen et al., 1992), and position 125 plays a somewhat larger role in stabilizing the isomaltose complex compared to maltose. It is not clear from the GA-acarbose crystal structures how the substitution of arginine with lysine, which has a similar but shorter basic side chain, could induce favorable interactions in the GA-isomaltose transition-state complex since Arg125 is removed from subsite 2.

Pro123→Gly. Preliminary kinetic assays performed at 45 °C with Pro123→Gly GA indicated that the enzyme is unstable at 45 °C even though wild-type GA under similar conditions is stable up to 60 °C. Residual enzymatic

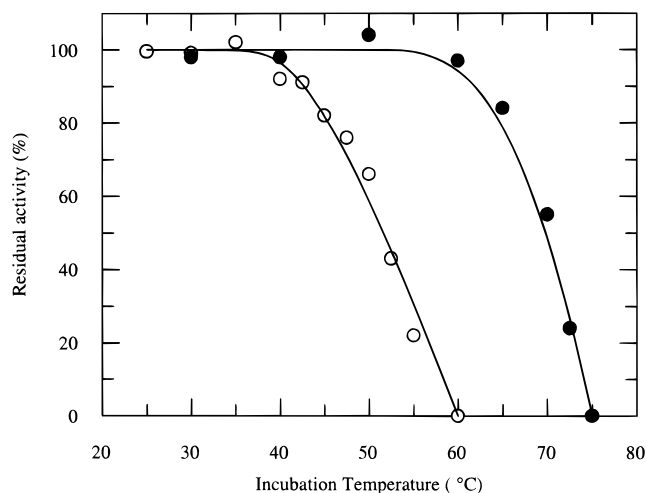


FIGURE 2: Irreversible thermal denaturation of wild-type (●) and Pro123→Gly (○) glucoamylases. Residual activities were determined by incubating the enzymes at the indicated temperatures for 10 min in 0.05 M sodium acetate buffer, pH 4.5, and assaying for activity in the same buffer using 20 mM maltose as substrate at 25 °C.

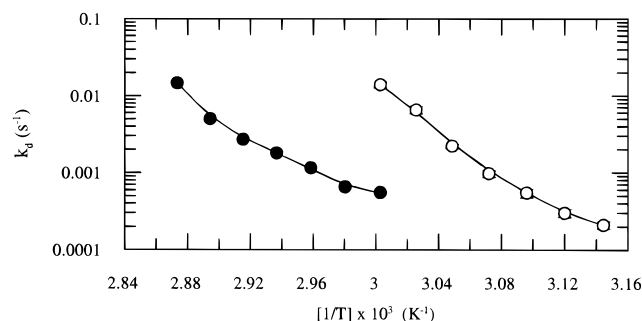


FIGURE 3: Temperature dependence of first-order irreversible denaturation rate, k_d , for wild-type (●) and Pro123→Gly (○) glucoamylases. Wild-type GA values were read from graphical data (Chen et al., 1994) with an estimated error of about 10%.

activities retained by Pro123→Gly and wild-type GAs after incubating for 10 min at different temperatures from 25 to 75 °C are shown in Figure 2. The irreversible denaturation temperature T_m , defined as the temperature at which the enzyme exhibits only 50% of the original activity, is 70 °C for the wild-type GA and 51 °C for Pro123→Gly, a 19 °C decrease due to the single proline to glycine substitution.

The first-order rate constants of irreversible denaturation, k_d , for wild-type and Pro123→Gly GAs are shown in Figure 3. The k_d values for Pro123→Gly GA in the temperature range 45–60 °C are fairly similar to k_d values for the wild type in the 60–75 °C range indicating that inactivation mechanisms for both the enzymes may be similar even though the decay process starts at a much lower temperature for the mutant. k_d values for wild-type GA in the 70–75 °C temperature range and for Pro123→Gly GA in the 55–

60 °C range agree particularly well. Unfolding of the tertiary structure is the dominant denaturation mechanism in wild-type GA at temperatures above 70 °C (Chen et al., 1994), and the mutant is likely to denature above 55 °C by a very similar mechanism.

The kinetic parameters for Pro123→Gly GA were determined at 25 °C (Table 2), a temperature for which the enzyme was stable during the time frame of the experiment. The kinetic parameters for maltose, maltotriose, and isomaltose are available for wild-type GA at 25 °C (Meagher et al., 1989a) and are also included in Table 2 for comparison. The k_{cat} values for the mutant enzyme with maltose, maltotriose, and isomaltose are about 35% less than wild type, while the K_{m} values were comparable. The slight decrease in k_{cat} values observed with the mutant GA are at least partly due to the denaturation of the enzyme during the fermentation at 30 °C and subsequent purification at 4 °C. The kinetic parameters for hydrolysis of the remainder of the maltooligosaccharide series with wild-type GA are not available in literature, so quantitative comparisons of the mutant data with these substrates cannot be made. Kinetic parameters for hydrolysis of the maltooligosaccharide series with wild-type GA, however, are available at 50 °C (Sierks et al., 1989), 45 °C (Table 1), 35 °C (Meagher et al., 1989b), and 8 °C (Olsen et al., 1993) and indicate consistent increases in k_{cat} and K_{m} for all substrates with increasing temperature. This same trend in kinetic parameters for maltooligosaccharide hydrolysis are noticed in the mutant enzyme at 25 °C. Accounting for a slight decrease in k_{cat} of the mutant enzyme due to denaturation during production, the kinetic constants obtained with the Pro123→Gly GA are very similar to those obtained with wild type indicating the active site of GA is not altered by the Pro123→Gly substitution. The large decrease in thermal stability is therefore attributable to local specific interactions resulting from the proline to glycine substitution.

Thermal Stability. Proline residues in nonstructural loops connecting secondary structures are important factors in determining thermal stability of proteins. The psychrophilic α -amylase from *Alteromonas haloplantis* has the lowest proline content found among α -amylases, where the prolines occurring in loops and turns of the thermophilic amylases are deleted or substituted by small amino acids such as alanines (Feller et al., 1994). The thermostability of oligo-1,6-glucosidase from *Bacillus thermoglucosidarius* has been correlated with the presence of additional proline residues occurring with high frequency in the loop regions (Watanabe et al., 1991). The pyrrolidine of proline restricts the protein backbone flexibility around this residue to a great extent. The substitution of proline by a more flexible amino acid residue like glycine or alanine can potentially decrease the thermal stability due to increased entropy of unfolding (Matthews et al., 1987). Protein stability studies undertaken with human lysozyme (Herning et al., 1992) and tryptophan synthase α -subunit (Yutani et al., 1991) suggest that the magnitude of the effect of proline residues from nonstructural loop regions on reversible denaturation is dependent on the accessibility and the mobility of the residue, where prolines with limited mobility and low accessibility have the largest effect on folding and stability. In the case of lysozyme, a conserved proline appears to be important for stability whereas nonconserved prolines do not (Herning et al., 1992). The increase in entropy of unfolding associated with all

Table 4: $k_{\text{cat}}/K_{\text{m}}$ Values for Wild-Type and Mutant Glucoamylases

enzyme	$k_{\text{cat}}/K_{\text{m}}$ ($\text{s}^{-1} \text{mM}^{-1}$)	
	α -D-glucosyl fluoride	maltose
wild type ^c	13.7 \pm 0.5	6.57 \pm 0.80
Tyr116→Ala ^{a,c}	13.8 \pm 1.4	0.93 \pm 0.12
Trp120→Phe ^c	12.6 \pm 0.5	0.25 \pm 0.06
Gly121→Thr ^c	11.7 \pm 0.4	2.6 \pm 0.19
Arg122→Tyr ^c	5.0 \pm 0.2	0.36 \pm 0.02
Gln124→His ^c	4.6 \pm 0.2	0.85 \pm 0.07
Arg125→Lys ^c	12.0 \pm 0.04	10.8 \pm 0.9
Wild type ^d	6.1 \pm 0.1	3.93 ^b
Pro123→Gly ^d	3.9 \pm 0.1	2.7 \pm 0.18

^a From Sierks and Svensson (manuscript submitted). ^b Value read from graphical data (Meagher et al., 1989a) with an estimated error of about 10%. ^c 45 °C. ^d 25 °C.

Pro→Gly mutations is therefore only partially responsible for a decrease in thermal stability, whereas specific local interactions are apparently more crucial.

Pro123, which is highly conserved in all the GAs and glucose oxidase, is part of a nonstructural loop immediately adjacent to the active center of the enzyme. The mean thermal factor B for Pro123 calculated from the GA crystallographic data (Aleshin et al., 1994a) is 3.06 Å². This low B value indicates a large configurational strain on the proline backbone. Only about 26% of the proline residue is exposed to the solvent as calculated from the GA structural data (Aleshin et al., 1994a) where only the side chain is accessible. The decrease in thermal stability of the Pro123→Gly mutation, a conserved proline with low mobility and accessibility, is consistent with the general trends seen in other enzymes although 19 °C is the highest change in thermal stability reported in literature for a single Pro→Gly mutation in a nonstructural protein region to our knowledge. Although GA unfolds irreversibly on heating (Williamson et al., 1992) whereas lysozyme and the tryptophan synthase α -subunit unfold reversibly, similar factors may play a role in both reversible and irreversible denaturation. Further studies with other temperature sensitive mutants are required to obtain a better understanding of the structural changes accompanying the denaturation process of GA.

α -D-Glucosyl Fluoride Kinetics. Two residues in the Trp120 loop region, Trp120 and Tyr116, have been shown to play important roles for maltose hydrolysis but rather insignificant roles for GF hydrolysis (Sierks & Svensson, 1996). This observation led to the hypothesis that release of the reducing end product from the GA active site is the rate-limiting step in the catalytic mechanism. To further explore this theory, GF was utilized as a substrate with the five mutations in the Trp120 region constructed in this study. The $k_{\text{cat}}/K_{\text{m}}$ values obtained with these enzymes and also with Trp120→Phe GA for α -D-glucosyl fluoride hydrolysis at 45 °C are given in Table 4.

The mutations Gly121→Thr, Pro123→Gly, and Arg125→Lys have relatively small effects on hydrolytic activity toward maltose where the $k_{\text{cat}}/K_{\text{m}}$ values were 40%, 65%, and 165% of the wild-type values, respectively. The $k_{\text{cat}}/K_{\text{m}}$ values obtained with GF as substrate for wild-type, Gly121→Thr, and Arg125→Lys GAs were essentially the same while $k_{\text{cat}}/K_{\text{m}}$ value for Pro123→Gly GA value was about 70% of the wild type. The loss in activity seen with the Pro123→Gly GA is most likely due to some enzyme denaturation during the production and purification process

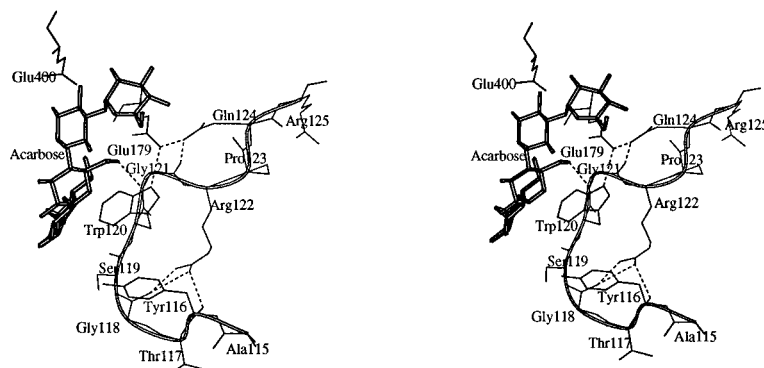


FIGURE 4: Stereoview of the active site of wild-type GA complexed with acarbose generated from the crystallographic coordinates of Aleshin et al. (1994b). The general catalytic acid (Glu179) and base (Glu400) groups and loop residues 115–125 are shown. Hydrogen bonds between donor–acceptor atoms within a distance of 3.3 Å are depicted by dashed lines. Only hydrogen bonding involving the Trp120 loop residues are shown for clarity. Illustration prepared using Molscript v1.4 (Kraulis, 1991).

as mentioned earlier, rather than to any effect on the catalytic mechanism.

The mutations Trp120→Phe, Arg122→Tyr, and Gln124→His had very significant effects on maltose hydrolysis decreasing $k_{\text{cat}}/K_{\text{m}}$ values about 26-, 18-, and 8-fold compared to wild type, respectively. With GF as substrate, however, the $k_{\text{cat}}/K_{\text{m}}$ value of Trp120→Phe GA is nearly the same as wild type, while Arg122→Tyr and Gln124→His GAs are only 2.6- and 3-fold less, respectively. Similar results were seen with Tyr116→Ala GA where $k_{\text{cat}}/K_{\text{m}}$ for maltose hydrolysis decreases 7-fold compared to wild type while the value for GF hydrolysis is the same as wild type (Sierks & Svensson, 1996). Mutations at residues 116, 120, 122, and 124 in the Trp120 loop region exhibit considerably lower activity towards maltose hydrolysis but similar activity toward GF hydrolysis compared to wild type, while mutations at residues 119 (Sierks & Svensson, 1994), 121, 123, and 125 do not substantially alter activity toward either substrate.

These results clearly indicate that the Trp120 loop residues play critical roles in maltooligosaccharide hydrolysis but only minor roles in GF hydrolysis. Maltooligosaccharide substrates may remain unproductively bound to GA even after the glycosidic bond cleavage as suggested (Kitahata et al., 1981; Sierks & Svensson, 1996) whereas GF has no such residue to slow down the reaction. This would account for the 50-fold faster turnover rate with GF than with maltose (Konstantinidis & Sinnott, 1991). The Trp120 loop residues, especially Tyr116, Trp120, Arg122, and Gln124, play crucial roles in releasing the different length reducing end products in the case of natural maltooligosaccharide substrates. The Arg122 and Tyr116 mutations have very distinct and qualitatively similar effects on activity with oligosaccharide substrates of different lengths. Both Arg122 and Tyr116 are likely to be actively involved in promoting activity toward short maltooligosaccharide substrates, presumably by facilitating release of the reducing end product.

Mechanistic Interpretations. The differences in the kinetic behavior of wild-type and the mutant GAs in this study toward GF and maltooligosaccharide substrates strongly suggest that reducing end product release is the rate-determining step in the GA mechanism and that the Trp120 loop residues play a critical role in that step. Residues Tyr116, Trp120, Arg122, and Gln124, in particular, are involved in liberating the products from the binding pocket of the enzyme. Substitution of these residues results in

significantly lower K_{m} and k_{cat} values than wild-type GA for short maltooligosaccharides and isomaltose. None of the Trp120 loop mutations has impaired bond cleaving capability as evidenced by retained wild-type activity toward GF, so the decrease in K_{m} values seen for maltooligosaccharide hydrolysis with these enzymes may reflect an increased accumulation of enzyme–product complexes, and the decrease in k_{cat} values would then reflect a reduced ability to release these bound products. The combination of a decrease in k_{cat} , K_{m} , and $k_{\text{cat}}/K_{\text{m}}$ values seen with these mutations increases the activation barrier for the rate-determining product release step and indicates that these residues are involved in both the formation of ground-state enzyme–product complexes as well as the transition-state enzyme–product complex. The nature of the interactions of the Trp120 loop residues in dissociating enzyme–product complexes is not yet clear. The crystal structure of the GA–acarbose complex shows that Trp120 is stacked up against the hydrophobic face of the third residue of acarbose (Aleshin et al., 1994b). This nonbonded interaction places the glucosidic linkage between the second and the third residue in a considerable amount of strain. Aleshin and co-workers have suggested that this strain may possibly promote the release of products after hydrolysis (Aleshin et al., 1994b). Since Trp84 of *S. fibuliger* α -amylase, the residue equivalent to Trp120 of GA, located at subsite 3 also plays a crucial role in releasing the product after hydrolysis (Matsui et al., 1991), this highly conserved loop region may play similar important roles in other related enzymes.

In contrast to kinetic studies which clearly show the importance of Tyr116 and Arg122 in the catalytic mechanism, the crystal structure of the enzyme complexed with acarbose (Aleshin et al., 1994b) does not show any contacts of these residues with the inhibitor. These residues are removed from the seat of the reaction giving no indication of a substantial involvement in substrate binding. Fluorescence spectroscopy studies, however, indicate that neither the crystal structure of the free nor the complexed enzyme is a true representative of the structure of the rate-limiting enzyme-bound intermediate in solution. Stopped-flow fluorescence spectroscopy studies indicate that GA–acarbose complex formation involves at least one more step than the substrate–enzyme complex formation (Olsen et al., 1993). The complexation of substrate and enzyme showed just one phase of fluorescence decrease attributable to two distinct steps, while the complexation of acarbose with enzyme

displayed two phases of opposite changes in the intrinsic fluorescence. The first phase was similar to that observed in substrate complexes followed by a unique phase which shows an increase in fluorescence. The increase in fluorescence in the second phase could possibly be due to a relaxation of the enzyme–acarbose complex formed during the first phase reversing the initial conformational changes. This observation is supported by the identical structures of the native and acarbose complexed forms of the enzyme (Aleshin et al., 1994b). The crystal structure of the complexed enzyme indicates that the fourth residue of acarbose does not have any nonbonded contacts up to a distance of 3.5 Å. There is therefore no crystallographic evidence for the existence of the fourth and more distant subsites in GA even though there is kinetic evidence for these subsites.

Even though the crystal structure of complexed GA does not show significant interactions between inhibitor and the residues Tyr116 and Arg122 in the Trp120 loop region, we propose that substrate binding initiates conformational changes in the loop thereby bringing these two residues to coordinate with Trp120 and participate in catalysis. Figure 4 shows the residues of Trp120 loop in the GA–acarbose complex crystal structure (Aleshin et al., 1994b). The side chains of even numbered residues 116, 118, 120, 122, and 124 are pointing in one direction while the side chains of odd numbered residues 115, 117, 119, 121, 123, and 125 are pointing in the opposite direction. The even numbered residues Tyr116 (Sierks & Svensson, 1996), Trp120 (Sierks et al., 1989; Svensson & Sierks, 1992; Sierks & Svensson, 1996), Arg122, and Gln124 play critical roles in the enzyme mechanism, while the role of Gly118 has not been studied yet. The odd numbered residues Ser119 (Sierks & Svensson, 1994), Gly121, Pro123, and Lys125 play only minor roles in the catalytic mechanism while the roles of Ala115 and Thr117 have not been investigated. We postulate that the Trp120 loop undergoes conformational changes upon substrate binding to generate substantial interactions between even numbered loop residues and substrate or product which are not observed in the ground-state crystal structure. The NH₂ atom of Arg122 is hydrogen-bonded to carbonyl oxygen of Tyr116 in the crystal structure of GA (Aleshin et al., 1994a) suggesting that the function of these two residues could be coordinated. Harris et al. (1993) indicate that the GA–1-deoxynojirimycin crystal structure provides no answer as to how the substrates and inhibitors purge water from the active site and suggest that transient conformational changes must exist during substrate or inhibitor binding to facilitate the flow of water out of the active site. Many enzymes are known to operate via this kind of induced fit mechanism for various reasons. In the case of the extensively studied tyrosyl-tRNA synthetase, the residues of a loop located at a distance from the active site in the crystal structure have been shown to play a significant role in catalysis as a result of substrate induced conformational changes (Fersht et al., 1988). This kind of mechanism would allow the substrates to freely enter an “open” active site and cover itself with certain residues in the intermediate ground-state and or transition-state complexes which otherwise would block entry of the substrate. Part of the substrate binding energy can be used to fuel some of these conformational changes (Fersht et al., 1988). GA may utilize such a mechanism to keep the very long side chain of Arg122 and the bulky Tyr116 from preventing active site access to the substrate.

Conclusion. The highly conserved Trp120 loop residues play an important role in formation of both ground-state and transition-state enzyme complexes of GA and also in thermal stability as evident from kinetic analyses using maltooligosaccharide substrates. The differences in the kinetic behavior of wild-type and mutant GAs toward GF and maltooligosaccharide substrates strongly suggest that the release of the reducing end product is the rate-limiting step in the GA mechanism and that residues Tyr116, Trp120, Arg122, and Gln124 play a critical role in this step. These even numbered Trp120 loop residues play a role in liberating the products from the active site of the enzyme, although the exact nature of the interactions at the molecular level is not yet clear. The crystal structures of GA and GA–acarbose complex indicate that two critical residues, Tyr116 and Arg122, are slightly removed from the reaction site. These structures are not true representatives of the rate-determining enzyme-bound intermediate and therefore do not provide full information about the mechanistic roles of these residues. We propose that the Trp120 loop undergoes conformational changes upon substrate binding to considerably increase the interaction of the even numbered residues with substrate and product.

ACKNOWLEDGMENT

We are grateful to Cetus Corporation for the gift of the glucoamylase gene, yeast expression vector and *S. cerevisiae* strain. We thank Dr. Alexander Scriabine (Miles Inc., Westhaven, CT) for the gift of acarbose and Professor Inge Lundt (Danish Technical Institute, Lyngby, Denmark) for the gift of α -D-glucosyl fluoride. We also thank Pedro Coutinho for help in accessible surface area calculations from crystallographic data.

REFERENCES

- Aleshin, A. E., Hoffman, C., Firsov, L. M., & Honzatko, R. B. (1994a) *J. Mol. Biol.* 238, 575–591.
- Aleshin, A. E., Firsov, L. M., & Honzatko, R. B. (1994b) *J. Biol. Chem.* 269, 15631–15639.
- Amemura, A., Chakraborty, R., Fujita, M., Noumi, T., & Futai, M. (1988) *J. Biol. Chem.* 263, 9271–9275.
- Chen, H., Bakir, U., Reilly, P. J., & Ford, C. (1994) *Biotechnol. Bioeng.* 43, 101–105.
- Clarke, A. J., & Svensson, B. (1984a) *Carlsberg Res. Commun.* 49, 111–122.
- Clarke, A. J., & Svensson, B. (1984b) *Carlsberg Res. Commun.* 49, 559–566.
- Cole, E. G., McCabe, P. J., Inlow, D., Gelfand, D. H., Ben-Bassat, A., & Innis, M. A. (1988) *Bio/Technology* 6, 417–421.
- Coutinho, P. M., & Reilly, P. J. (1994) *Protein Eng.* 7, 749–760.
- Diderichsen, B., & Christiansen, L. (1988) *FEMS Microbiol. Lett.* 255, 37–41.
- Feller, G., Payan, G., Theys, F., Qian, M., Haser, R., & Gerday, C. (1994) *Eur. J. Biochem.* 222, 441–447.
- Fersht, A. (1985) *Enzyme Structure and Mechanism*, 2nd ed., W. H. Freeman, New York.
- Fersht, A. R., Knill-Jones, J. W., Bedouelle, H., & Winter, G. (1988) *Biochemistry* 27, 1581–1587.
- Fox, J. D., & Robyt, J. F. (1991) *Anal. Biochem.* 195, 93–96.
- Frandsen, T. P., Dupont, C., Lehmbeck, J., Stoffer, B., Sierks, M. R., Honzatko, R., & Svensson, B. (1994) *Biochemistry* 33, 13808–13816.
- Fredrick, K. R., Tung, J., Emerick, R. S., Masiaz, F. R., Chamberlain, S. H., Vasavada, A., & Rosenberg, S. (1990) *J. Biol. Chem.* 265, 2793–3802.
- Harris, E. M. S., Aleshin, A. E., Firsov, L. M., & Honzatko, R. B. (1993) *Biochemistry* 32, 1618–1626.

- Hecht, H. J., Kalisz, H. M., Hendle, J., Schmid, R. D., & Schomberg, D. (1993) *J. Mol. Biol.* 229, 153–162.
- Henrissat, B., Coutinho, P. M., & Reilly, P. J. (1994) *Protein Eng.* 7, 1281–1286.
- Herning, T., Yutani, K., Inaka, K., Kuroki, R., Matsuhima, M., & Kikuchi, M. (1992) *Biochemistry* 31, 7077–7085.
- Hiromi, K. (1970) *Biochim. Biophys. Acta* 40, 1–6.
- Hiromi, K., Kawai, M., & Ono, S. (1966a) *J. Biochem. (Tokyo)* 59, 476–480.
- Hiromi, K., Takahashi, K., Hamauzu, Z., & Ono, S. (1966b) *J. Biochem. (Tokyo)* 59, 476–480.
- Hiromi, K., Ohnishi, M., & Tanaka, A. (1983) *Mol. Cell. Biochem.* 51, 79–95.
- Ito, H., Fukuda, Y., Murata, K., & Kimura, A. (1983) *J. Bacteriol.* 153, 163–168.
- Itoh, T., Ohtsuki, I., Yamashita, I., & Fukui, S. (1987) *J. Bacteriol.* 169, 4171–4176.
- Jespersen, H. M., MacGregor, E. A., Henrissat, B., Sierks, M. R., & Svensson, B. (1993) *J. Protein. Chem.* 12, 791–805.
- Katsuragi, N., Takizawa, N., & Murooka, Y. (1987) *J. Bacteriol.* 169, 2301–2306.
- Kitahata, S., Brewer, C. F., Genghof, D. S., Sawai, T., & Hehre, E. J. (1981) *J. Biol. Chem.* 256, 6017–6026.
- Klein, C., & Schulz, G. E. (1991) *J. Mol. Biol.* 217, 737–750.
- Konstantinidis, A., & Sinnott, M. L. (1991) *J. Biochem. (Tokyo)* 279, 587–593.
- Kraulis, P. J. (1991) *J. Appl. Crystallogr.* 24, 946–950.
- László, E., Holló, J., Hoschke, A., & Sárosi, G. (1978) *Carbohydr. Res.* 61, 387–394.
- Leatherbarrow, R. J. (1992) *Grafit*, Version 3.0, Erithacus Software Ltd., Staines, U.K.
- Lee, D. D., Lee, Y. Y., Reilly, P. J., Collins, E. V., & Tsao, G. T. (1976) *Biotechnol. Bioeng.* 18, 253–287.
- Matsui, I., Ishikawa, K., Miyari, S., Fukui, S., & Honda, K. (1991) *Biochim. Biophys. Acta* 1077, 416–419.
- Matsuura, Y., Kusunoki, M., Harada, W., & Kakudo, M. (1984) *J. Biochem. (Tokyo)* 95, 697–702.
- Matthews, B. W., Nicholson, H., & Becktel, W. J. (1987) *Proc. Natl. Acad. Sci. U.S.A.* 84, 6663–6667.
- McGregor, E. A., & Svensson, B. (1989) *Biochem. J.* 259, 145–152.
- Meagher, M. M., & Reilly, P. J. (1989) *Biotechnol. Bioeng.* 34, 689–693.
- Meagher, M. M., Nikolov, Z. L., & Reilly, P. J. (1989) *Biotechnol. Bioeng.* 34, 681–688.
- Olsen, K., Svensson, B., & Christensen, U. (1992) *Eur. J. Biochem.* 209, 777–784.
- Olsen, K., Christiansen, U., Sierks, M. R., & Svensson, B. (1993) *Biochemistry* 32, 9686–9693.
- Palczic, M., Skrydstrup, T., Bock, K., Le, N., & Lemieux, R. U. (1993) *Carbohydr. Res.* 250., 87–92.
- Sanger, F., Nicklen, S., & Coulson, A. R. (1977) *Proc. Natl. Acad. Sci. U.S.A.* 74, 5463–5467.
- Savel'ev, A. N., & Firsov, L. M. (1982) *Biokhimiya* 47, 1618–1620.
- Sierks, M. R., & Svensson, B. (1994) *Protein Eng.* 7, 1479–1484.
- Sierks, M. R., & Svensson, B. (1996) *Biochemistry* (in press).
- Sierks, M. R., Ford, C., Reilly, P. J., & Svensson, B. (1989) *Protein Eng.* 2, 621–625.
- Sierks, M. R., Ford, C., Reilly, P. J., & Svensson, B. (1990) *Protein Eng.* 3, 193–198.
- Sierks, M. R., Bock, K., Refn, S., & Svensson, B. (1992) *Biochemistry* 31, 8972–8977.
- Svensson, B. (1988) *FEBS Lett.* 230, 72–76.
- Svensson, B., & Sierks, M. R. (1992) *Carbohydr. Res.* 227, 29–44.
- Svensson, B., Larsen, K., Svendsen, I., & Boel, E. (1983) *Carlsberg Res. Commun.* 48, 529–544.
- Watanabe, K., Chishiro, K., Kitamura, K., & Suzuki, Y. (1991) *J. Biol. Chem.* 266, 24287–24294.
- Wilkinson, A. J., Fersht, A. R., Blow, D. M., & Winter, G. (1983) *Biochemistry* 22, 3581–3586.
- Williamson, G., Belshaw, N. J., Noel, T. R., Ring, S. G., & Williamson, M. P. (1992) *Eur. J. Biochem.* 207, 661–670.
- Yutani, K., Hayashi, S., Sugisaki, Y., & Ogasahara, K. (1991) *Proteins: Struct., Funct., Genet.* 9, 90–98.

BI952458X